A Novel Fast Process for Zn(O,S) Buffer Layers, Doped With Al and B and Deposited on CIGSSe Solar Cells

C. Hönes, J. Hackenberg, R. Keller, S. Zweigart, A. Fuchs, and S. Siebentritt

***Abstract*—In the search for a nontoxic replacement of the commonly employed CdS buffer layer for Cu(In,Ga)(S,Se)$_2$ based solar cells, chemically deposited Zn(O,S) thin films are a most promising choice. In this paper, we address the usually slow deposition speed of Zn(O,S) in a newly developed ammonia-free chemical bath process, resulting in a deposition of 30 nm in 3 min with good homogeneity on 30 cm × 30 cm sized substrates. Solar cells with buffer layers prepared from this process match the efficiency of CdS reference cells. In a second step, we address the light-soaking post-treatment, still needed for maximum efficiencies. By addition of aluminum to the deposition process, the initial efficiencies can be increased slightly. With the addition of boron, the light-soaking post-treatment is rendered unnecessary, while maintaining high efficiencies above 15%, surpassing reference cells with CdS buffer.**

***Index Terms*—Buffer layers, chemical bath deposition, CIGS thin film solar cells, photovoltaic cells, zinc oxysulfide.**

I. Introduction

CHALCOPYRITE Cu(In,Ga)Se$_2$ and Cu(In,Ga)(S,Se)$_2$ (CIGSSe) based solar cells reached efficiencies as high as 22.6% in the recent past [1]. Most highly efficient cells are produced with toxic cadmium sulfide buffer layers [2], [3]. There was, however, some progress in the development of alternative cadmium-free buffer layers with layers based on zinc oxysulfide Zn(O,S) to be a most promising example, reaching efficiencies up to 21% on cell level [4] and 17.9% on 30 cm × 30 cm submodule level [5]. Processes for Zn(O,S) thin film deposition usually contain ammonia as complexing agent and for pH control, and thiourea or thioacetamide as sulfur source. In addition to zinc sulfide and zinc oxide formation, the chemistry of these chemical bath deposition (CBD) processes usually also leads to zinc hydroxide formation [6], and the resulting buffer layers are therefore sometimes referred to as Zn(O,OH,S) buffer layers. For the sake of simplicity, we will use the nomenclature of Zn(O,S) in the following.

Regarding the deposition time, thiourea-based processes are usually slow, taking up to 20 min for a deposition of 30 nm [5]–[7]. This time can be reduced to 5–8 min by working with preheated reagents [6] or by replacing thiourea with faster decomposing thioamides [8], [9]. If thioacetamide is used as replacement for thiourea, the precipitation reaction is even too fast, making it necessary to replace part of the ammonia by another, stronger complexing agent [8]. Apart from faster film formation, the latter approach also has the advantage of lowering the amount of ammonia, which is advantageous for industrial processes, where exhaust gas has to be cleaned from ammonia fumes. In this paper, we therefore concentrate on the development of an altogether ammonia-free deposition process, where we use ammonia containing solutions only for established pre and posttreatment steps. This novel process utilizes N-(2-hydroxyethyl)ethylenediaminetriacetic acid (HEEDTA) as complexing agent at high pH, controlled with NaOH, and thioacetamide as sulfur source. This deposition process is not only faster compared with previously published processes, but also uses lower concentrations of chemicals, potentially reducing fabrication costs.

A common disadvantage of Zn(O,S) buffer layers is the need for light-soaking treatments after cell preparation in order to achieve metastable maximum efficiencies. This behavior is attributed to an electronic barrier between CIGSSe absorber and n-type window layer and can be addressed by adjusting the [S]/([S]+[O]) ratio of the Zn(O,S) layer or by introducing indium to be another cation, both lowering the positive conduction band offset (spike) at the CIGSSe/buffer interface [10], [11]. Alternatively, the common i-ZnO high resistive window layer can be replaced with ZnMgO or the n-type doping of the buffer layer can be increased [12].

Regarding the latter approach, we additionally examine the possibility of doping the buffer layer with Al and B. It has been shown that it is possible to use aluminum as n-type dopant for ZnS thin films [13], [14]. It was also shown by Khallaf *et al.* that doping of CdS layers within a common CBD process is possible by means of adding aluminum sulfate or boric acid to the process solution [15], [16]. We therefore pursue the same approach here.

Manuscript received October 16, 2016; revised December 6, 2016 and January 21, 2017; accepted February 8, 2017. Date of publication March 7, 2017; date of current version April 19, 2017.

C. Hönes is with Robert Bosch GmbH, Engineering Sensor Process Technology, Reutlingen 72762, Germany, and also with the Laboratory for Photovoltaics, University of Luxembourg, Belvaux 4422, Luxembourg (e-mail: christian.hoenes@de.bosch.com).

J. Hackenberg, R. Keller, S. Zweigart, and A. Fuchs are with Robert Bosch GmbH, Corporate Research and Advance Engineering, Renningen 71272, Germany (e-mail: juergen.hackenberg@de.bosch.com; rolfd.keller@de.bosch.com; siegmund.zweigart@de.bosch.com; anne.fuchs@de.bosch.com).

S. Siebentritt is with the Laboratory for Photovoltaics, University of Luxembourg, Belvaux 4422, Luxembourg (e-mail: susanne.siebentritt@uni.lu).

Color versions of one or more of the figures in this paper are available online at http://ieeexplore.ieee.org.

Digital Object Identifier 10.1109/JPHOTOV.2017.2669360

II. Experimental Procedure

For this paper, Zn(O,S) buffer layers were deposited in an alkaline CBD process on top of $Cu(In,Ga)(S,Se)_2$ absorber material. The latter was deposited on molybdenum coated soda lime glass in a large area process described elsewhere [17]. From the center area of each large area substrate, three neighboring pieces with dimension 30 cm $\times$ 30 cm were cut and used for the deposition processes presented in this paper. The equipment utilized for deposition processes consists of a deposition chamber, where substrates of 30 cm $\times$ 30 cm size are heated from one side with constant water flow and are exposed to the process chamber containing process solutions on the other side. During deposition, the whole setup is set in motion, ensuring a constant mixing of the solutions in the process chamber. The sample processing consists of three steps, a pretreatment, the actual Zn(O,S) deposition, and a cleaning step. During the pretreatment, the process chamber contains 2.5% ammonia solution, containing 15 mM HEEDTA, and the substrate temperature is raised to 75 °C, a process taking 5 min. After dumping the pretreatment solution, and rinsing the substrate with deionized water, a preheated process solution is transferred to the process chamber. This solution contains 5 mM $Zn(SO)_4$, 15 mM HEEDTA, 0.56 M NaOH, and 10 mM thioacetamide, dissolved in deionized water. The thioacetamide is added after preheating the process solution to 75 °C, directly before transferring to the process chamber. A volume of 400 mL was found to be sufficient in order to have a homogeneous deposition process on 30 cm $\times$ 30 cm substrates. The temperature was kept at 75 °C during deposition and the deposition time, typically between 2 and 5 min, depends on the target layer thickness and on the absorber surface conditions, and was fixed to 3 min for the experiments presented here. The cleaning step consists of a washing in 2.5% ammonia solution, removing loosely attached precipitates. After drying the sample in nitrogen gas flow, it is submitted to a heat-treatment at 190 °C for 10 min in air.

In order to intentionally dope the Zn(O,S) layers with aluminum or boron, aluminum potassium sulfate dodecahydrate or boric acid were added to the process solution with concentrations of 1 and 12.5 mM, respectively.

CIGSSe substrates from the same fabrication batch with a CdS buffer layer, already deposited at CISTech GmbH, were used for the preparation of reference cells.

For solar cell preparation, pieces with the dimension of 3.5 cm $\times$ 7 cm were cut from the larger substrate. The actual cells were then prepared at the Zentrum für Solarenergie- und Wasserstoff–Forschung Baden Württemberg (ZSW) with a sputtered intrinsic zinc oxide layer, followed by an aluminum-doped zinc oxide layer and a Ni/Al contact grid. Mechanical scribing leads to separated cells with an area of 0.5 cm^2 in an array of 2 $\times$ 10 cells per substrate. All cells presented here were prepared without an antireflection coating. Current–voltage (J–V) measurements were performed in the dark and under simulated AM1.5 illumination at the ZSW. Each cell is measured before any posttreatment, after annealing at 200 °C in air, and after light-soaking under simulated AM1.5 illumination for 30 min. During the measurements and during light-soaking, the cells were actively cooled to 25 °C.

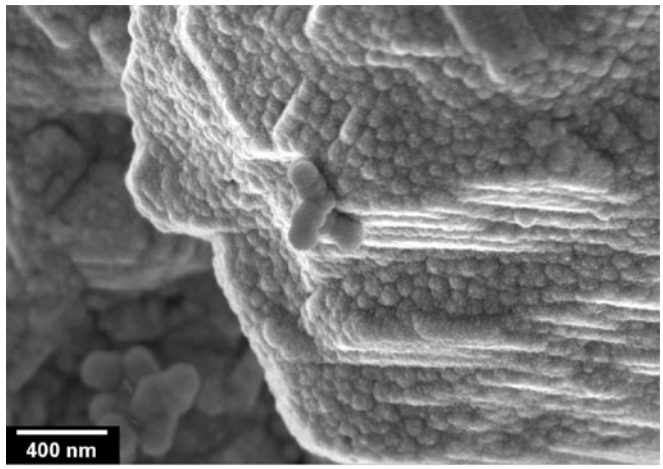

(a)

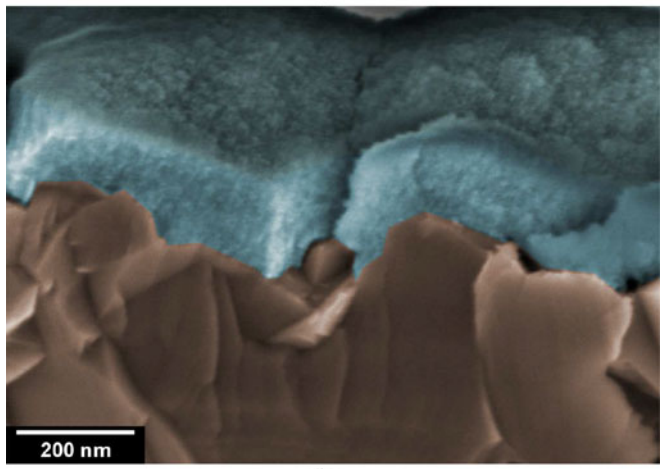

(b)

Fig. 1. SEM images for CIGSSe/Zn(O,S) layer stacks, showing (a) the surface morphology of a Zn(O,S) film after a single CBD deposition process and (b) a colorized cross section of a Zn(O,S) film from two prolonged consecutive CBD processes in order to achieve a higher film thickness.

Zn(O,S) layer thicknesses were controlled by means of X-ray fluorescence (XRF) measurements using a Fischerscope X-RAY XDV-SDD instrument. Scanning electron microscopy (SEM) images, shown in this paper, were taken at the CISTech GmbH facilities. X-ray photoelectron spectroscopy (XPS) measurements were performed using a Physical Electronics Quantera SXM instrument, equipped with a monochromatic Al anode.

III. Results and Discussion

A. Film Properties

The process described in the experimental section leads to very fast Zn(O,S) film formation. Film formation starts before the process solution is beginning to become turbid, which is an indicator for a fast surface catalyzed reaction, where the HEEDTA-complex with its single hydroxyl group might be the key component. The resulting film looks as if it consists of closely packed small spheres and exhibits good step coverage and low density of pin-holes, as can be seen in the SEM images shown in Fig. 1. Also visible in the image are some small

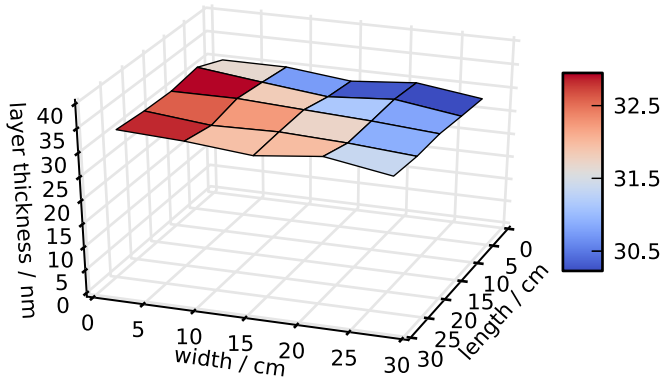

Fig. 2. XRF thickness map of an exemplary Zn(O,S) buffer layer deposited on a 30 cm × 30 cm CIGSSe substrate.

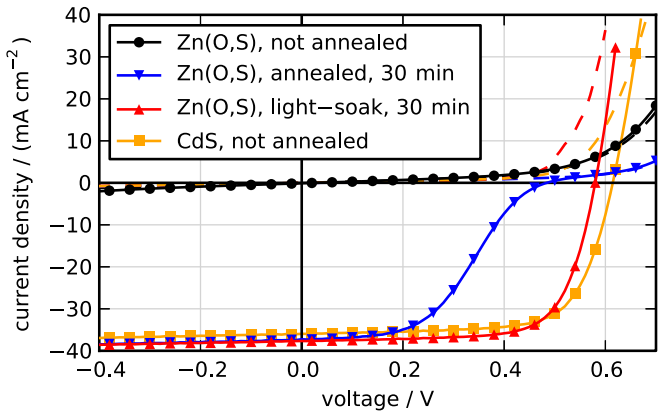

Fig. 3. J–V curves for an exemplary solar cell with Zn(O,S) buffer layer before annealing, after annealing for 30 min at 200 °C and after light-soaking for 30 min under simulated AM1.5 illumination in comparison to a reference cell with CdS buffer layer.

spherical agglomerates attached to the surface. These agglomerates can be found on the entire surface and probably stem from the homogeneous precipitation of Zn(O,S) in the process solution. A SEM cross section, displayed in Fig. 1(b), shows that the film does not show a clear grain or particle structure.

Regarding the suitability of the presented CBD process for large area deposition, a map of the film thickness, measured by XRF over 25 cm × 25 cm, is shown in Fig. 2. Despite the short process time, the layer formation is very homogeneous on a large substrate area, with relative standard deviations for the layer thickness usually being below 5%.

B. Solar Cells

A typical example of measured J–V curves is displayed in Fig. 3. Clearly, these devices show a light-soaking behavior, which is commonly observed for cells with Zn(O,S) buffer layers [18]. Before any posttreatment, there is no significant short circuit current density (J_{SC}), and therefore no efficiency (η). After the annealing posttreatment, the cells show some efficiency, which is, however, still limited because of a large S-shape distortion of the J–V curve. After the following light-soaking posttreatment, the cells reach their maximum efficiency, showing no S-shape distortion of the J–V curve any more. Statistical data, involving six samples from separate CBD deposition processes on similar CIGSSe material in comparison with reference CdS layers, are presented in Table I and Fig. 4. Each sample contains 20 solar cells, out of which only 10 are measured before light-soaking. The number of measured cells is given by n in the table. It is apparent that the presented process results in Zn(O,S) buffer layers that match the efficiency of CdS references. It is also apparent from the plot in Fig. 4 and from the printed median absolute deviations that the deviation of solar cell parameters is on the same level. Although the efficiency matches the reference cells, there is still a significant loss in open circuit voltage (V_{OC}), counterbalanced by gains in J_{SC} and fill factor. The gain in J_{SC} is expected as Zn(O,S) thin films have a larger band gap compared with CdS thin films. The lower V_{OC} is commonly observed for cells with Zn(O,S) buffer layer [4], [7], while the reason for this deficiency is still in the dark. Recent results presented by Hariskos *et al.* however show that it is possible to reach high open circuit voltages with a Zn(O,S) buffer layer deposited by an thiourea-based CBD process [8]. The slightly higher fill factor for the cells with Zn(O,S) buffer layer in Table I on the other hand can be explained by the fact that the reference cells were not put to the light-soaking treatment. A slightly increased fill factor is sometimes observed as result of such a treatment even for our reference cells. The active cell area, after subtracting the grid area, is 0.47 cm^2 for all cells presented here. The maximum active area efficiency of cells with standard Zn(O,S) buffer from the process reported here is therefore calculated to be 16.1%.

TABLE I
SOLAR CELL PARAMETERS AFTER ANNEALING AND AFTER LIGHT-SOAKING. STATISTICAL DATA IS REPRESENTED BY ITS MEDIAN AND MEDIAN ABSOLUTE DEVIATION. THE NUMBER OF CELLS IS GIVEN BY n

	buffer layer		
parameter	Zn(O,S) annealed	Zn(O,S) light-soaked	CdS
n	60	120	60
η / %	6.89 ± 2.32	14.92 ± 0.29	14.45 ± 0.48
η_{max} / %	13.3	15.5	15.6
V_{OC} / mV	453 ± 63	567 ± 6	607 ± 2
fill factor / %	39.2 ± 8.7	69.6 ± 0.9	66.6 ± 1.6
J_{SC} / mA cm^{-2}	37.3 ± 0.6	37.7 ± 0.3	36.1 ± 0.1

C. Doping With Al and B

With the aim of lowering the need for a light-soaking posttreatment, it is attempted here to increase the n-type doping concentration in the buffer layer. As described in the experimental section, intentional doping with aluminum or boron is attempted by addition of $\mathrm{AlK(SO_4)_2 \cdot 12H_2O}$ or boric acid ($\mathrm{B(OH)_3}$) to the process solution. Within the described concentrations, both substances do not alter the deposition process in any manner. There is, however, a distinct influence on the solar cell parameters of solar cells produced from these altered solution formulations. Boxplots of the efficiencies before and after each posttreatment

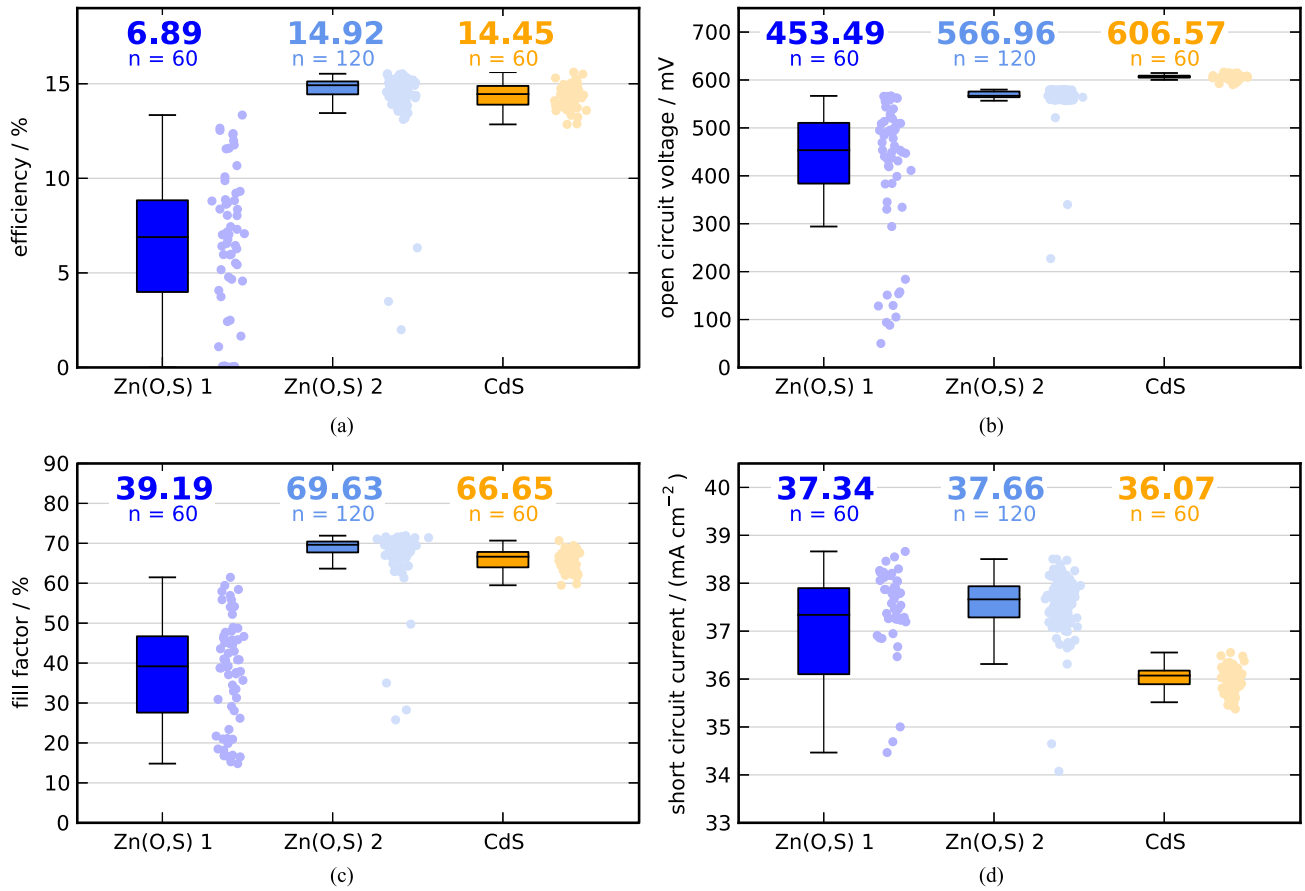

Fig. 4. Boxplots of solar cell parameters for cells with Zn(O,S) buffer layer after annealing (1) and after light-soaking (2) in comparison with cells with CdS buffer layer. Median values are given above each boxplot together with the number of cells in the dataset. Scatter plot of the dataset are drawn next to each boxplot.

are shown in comparison to Zn(O,S) reference layers in Fig. 5. The performance of these reference cells differs slightly from the performance of those presented earlier, because of small variations between different CIGSSe material batches. In the case of added aluminum salt, a slight increase in efficiency is noted before and after any posttreatment. It has to be noted here that this slight increase, although significant in some batches, is not apparent in others. However, with added boric acid, the increase in efficiency is large and was observed reproducibly. The maximum efficiency of a cell with Zn(O,S):B buffer layer was measured to be 15.9% (16.9% on active area). The gain in efficiency is in both cases mostly caused by a shift of the S-shape to the right, indicating a reduction of the electronic barrier between absorber and window layer. With added boric acid, the solar cells do not show any significant light-soaking behavior any more. While the untreated cells show already larger efficiencies indicating a smaller electronic barrier to the current, this barrier is removed with the annealing posttreatment. There are many reasons for a possible reduction of this electronic barrier, an increase in buffer layer conductivity because of n-type doping among them [12], [19]. The increased electron density in the buffer layer puts the Fermi level closer to the conduction band at the absorber/buffer interface, facilitating thermionic charge transfer at this interface in the presence of a positive conduction band offset. Although the amounts of aluminum salt and boric acid added to the solution are large, there was no boron or aluminum detected in the layers by means of XPS. The sensitivity of XPS for detection of aluminum or boron is in the range of a few atomic percent, giving an upper bound to the possible incorporation. A closer look at the surface valence band spectra of intentionally doped layers compared with a reference layer shows a systematic increase of the difference between the valence band maximum energy and the Fermi level, as displayed in Fig. 6. Even if we assume that the thin buffer layer is largely depleted, being in contact with the depletion zone of the absorber, this might be an indicator of higher n-type doping in the buffer layer. The difference in $|E_{\mathrm{VBM}} - E_{\mathrm{F}}|$ from reference to boron doped layer is as large as 0.27eV. Apart from the donor concentration in the buffer layer, there might be an additional influence of the conduction band offset at the absorber/buffer interface on the electronic barrier. With Zn(O,S), it is possible to lower this offset by lowering the ratio [S]/([S+O]) of the material. In Table II, this ratio is displayed together with the mentioned Fermi level shift. For the calculation, we use atomic concentrations derived from integral peak intensities after a short sputter step as well as the Zn Auger parameter according to Adler *et al.* [20]. For both methods of calculation and for all layers, the ratios [S]/([S+O])$\sim$0.65 are very similar. An unintentional alteration of the conduction band offset bacause of a change in the anion ratio is therefore unlikely.

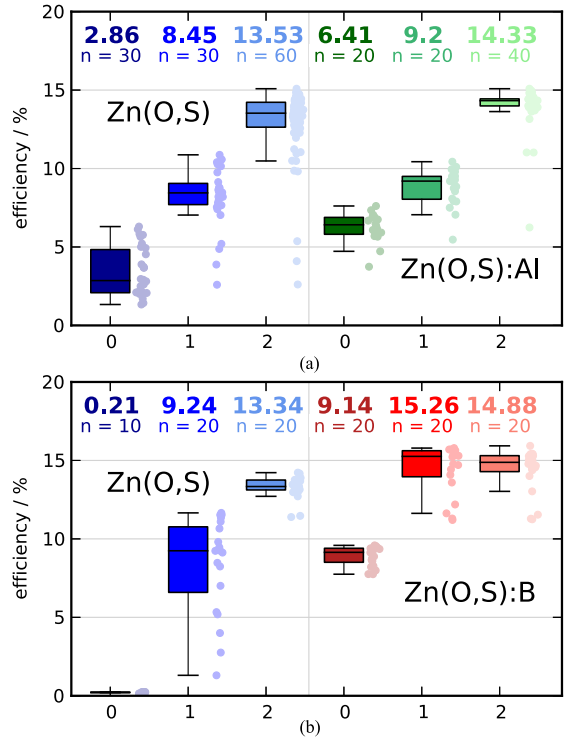

Fig. 5. Boxplots of solar cell efficiencies for Zn(O,S) buffer layers intentionally doped with (a) Al or (b) B in comparison with reference devices without intentional doping before annealing (0), after annealing (1) and after light-soaking (2). Median values are given above each boxplot together with the number of cells in the dataset. Scatter plot of the dataset are drawn next to each boxplot.

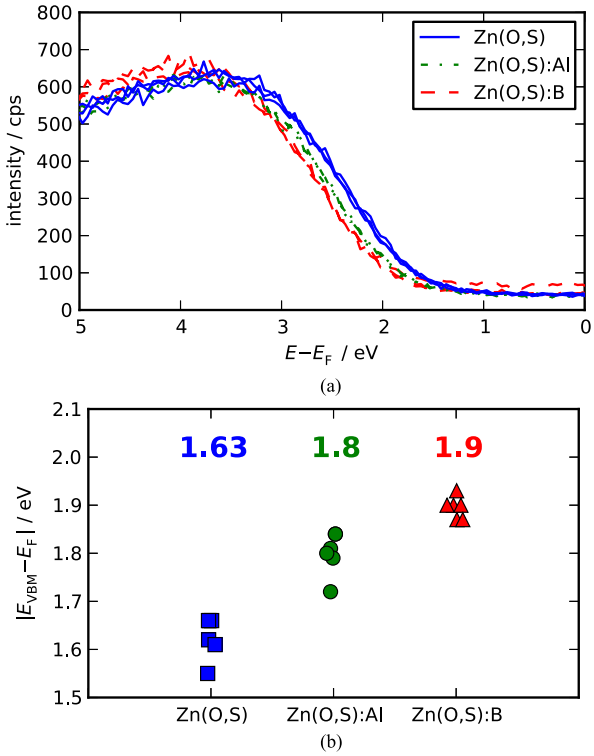

Fig. 6. Results from XPS surface measurements on CIGSSe/Zn(O,S) layer stacks without and with intentional doping of the buffer layer: (a) valence band spectra and (b) extrapolated valence band maximum energies. The datasets are measured on the same sample at different locations.

TABLE II
LAYER PROPERTIES DERIVED FROM XPS MEASUREMENTS

	buffer layer		
parameter	Zn(O,S)	Zn(O,S):Al	Zn(O,S):B
[S]/([S+O]) (atomic concentration)	0.65	0.66	0.66
[S]/([S+O]) (Auger parameter)	0.62	0.65	0.67
$\lvert E_{\mathrm{VBM}} - E_{\mathrm{F}} \rvert$/eV	1.63	1.80	1.90

IV. CONCLUSION

In this paper, we presented a novel, fast, and ammonia-free deposition process for Zn(O,S) buffer layers. The deposition step itself takes only 3 min and the layers show good step coverage, low density of pin-holes, and homogeneous thickness on 30 cm × 30 cm sized CIGSSe substrates. After annealing and a light-soaking posttreatment, the efficiencies of prepared solar cells match or even surpass those of prepared CdS reference devices and show good reproducibility. Adding $AlK(SO_4)_2 \cdot 12H_2O$ or boric acid to the process solution can improve the light-soaking behavior, slightly in the former case, significantly in the latter case. The maximum efficiency for CIGSSe solar cells with cadmium-free buffer layer from our lab is presented here with 16.9% active area efficiency for a Zn(O,S):B buffer layer. Although neither aluminum nor boron have been directly traced in this paper (additional secondary ion mass spectrometry measurements were inconclusive), the change in valence band offset is an indicator that the electronic structure of the buffer layer really is changed by the addition of aluminum salt or boric acid. And, not least, the improved solar cell efficiencies and light-soaking behavior should motivate to further pursue this route of deposition for Zn(O,S) buffer layers.

The results presented here therefore constitute an important step forward in the search for a fast and reliable fabrication method for chemically deposited Zn(O,S) buffer layers.

ACKNOWLEDGMENT

The authors would like to thank A. Wachau, F. Stober, F. Hergert, and the Bosch Solar CISTech GmbH for supplying them with $Cu(In,Ga)(S,Se)_2$ absorber material and SEM images of layers deposited by the authors, and for valuable discussions on the topic of cadmium-free buffer layers in general. They would also like to thank S. Spiering and the Zentrum für Sonnenenergie- und Wasserstoff–Forschung Baden–Württemberg for the deposition of window layers and current–voltage measurements.

REFERENCES

[1] P. Jackson *et al.*, "Effects of heavy alkali elements in $Cu(In,Ga)Se_2$ solar cells with efficiencies up to 22.6%," *Physica Status Solidi (RRL)—Rapid Res. Lett.*, vol. 10, no. 8, pp. 583–586, 2016.

[2] P. Jackson *et al.*, "Properties of $Cu(In,Ga)Se_2$ solar cells with new record efficiencies up to 21.7%," *Physica Status Solidi (RRL) — Rapid Res. Lett.*, vol. 9, no. 1, pp. 28–31, 2015.

[3] P. Reinhard *et al.*, "$Cu(In,Ga)Se_2$ Thin-film solar cells and modules—A boost in efficiency due to potassium," *IEEE J. Photovolt.*, vol. 5, no. 2, pp. 656–663, Mar. 2015.

[4] T. M. Friedlmeier *et al.*, "Improved photocurrent in Cu(In,Ga)Se_2 solar cells: From 20.8% to 21.7% efficiency with CdS buffer and 21.0% Cd-free," *IEEE J. Photovolt.*, vol. 5, no. 5, pp. 1487–1491, Sep. 2015.

[5] J. Nam *et al.*, "Achievement of 17.9% efficiency in 30 $\times$ 30 cm^2 Cu(In,Ga)(Se,S)$_2$ solar cell sub-module by sulfurization after selenization with Cd-free buffer," *Prog. Photovolt., Res. Appl.*, vol. 24, no. 2, pp. 175–182, 2015.

[6] C. Hubert *et al.*, "The Zn(S,O,OH)/ZnMgO buffer in thin film Cu (In,Ga)(S,Se)$_2$-based solar cells part I: Fast chemical bath deposition of Zn(S,O,OH) buffer layers for industrial application on Co-evaporated Cu(In,Ga)Se_2 and electrodeposited CuIn(S,Se)$_2$ solar cells," *Prog. Photovolt., Res. Appl.*, vol. 17, no. 7, pp. 470–478, 2009.

[7] D. Hariskos *et al.*, "New reaction kinetics for a high-rate chemical bath deposition of the Zn(S,O) buffer layer for Cu (In,Ga)Se_2-based solar cells," *Prog. Photovolt., Res. Appl.*, vol. 20, no. 5, pp. 534–542, 2012.

[8] D. Hariskos *et al.*, "Method for a high-rate solution deposition of Zn(O,S) buffer layer for high-efficiency Cu(In,Ga)Se_2 -based solar cells," *IEEE J. Photovolt.*, vol. 6, no. 5, pp. 1321–1326, Sep. 2016.

[9] J. Löckinger *et al.*, "New sulphide precursors for Zn(O,S) buffer layers in Cu(In,Ga)Se_2 solar cells for faster reaction kinetics," *J. Opt.*, vol. 18, no. 8, 2016, Art. no. 084002.

[10] C. Platzer-Björkman *et al.*, "Zn(O,S) buffer layers by atomic layer deposition in Cu(In,Ga)Se_2 based thin film solar cells: Band alignment and sulfur gradient," *J. Appl. Phys.*, vol. 100, 2006, Art. no. 044506.

[11] C. Hönes, A. Fuchs, S. Zweigart, and S. Siebentritt, "Improved chemically deposited Zn(O,S) buffers for Cu(In,Ga)(S,Se)$_2$ solar cells by controlled incorporation of indium," *IEEE J. Photovolt.*, vol. 6, no. 1, pp. 319–325, Jan. 2016.

[12] N. Naghavi, S. Temgoua, T. Hildebrandt, J. F. Guillemoles, and D. Lincot, "Impact of oxygen concentration during the deposition of window layers on lowering the metastability effects in Cu(In,Ga)Se_2/CBD Zn(S,O) based solar cell," *Prog. Photovolt., Res. Appl.*, vol. 23, no. 12, pp. 1820–1827, 2015.

[13] J. Liao, S. Cheng, H. Zhou, and B. Long, "Al-doped ZnS thin films for buffer layers of solar cells prepared by chemical bath deposition," *Micro Nano Lett.*, vol. 8, no. 4, pp. 211–214, 2013.

[14] P. Prathap, N. Revathi, Y. Subbaiah, K. R. Reddy, and R. Miles, "Preparation and characterization of transparent conducting ZnS:Al films," *Solid State Sci.*, vol. 11, no. 1, pp. 224–232, 2009.

[15] H. Khallaf *et al.*, "In-situ boron doping of chemical-bath deposited CDS thin films," *Physica Status Solidi (a)*, vol. 206, no. 2, pp. 256–262, 2009.

[16] H. Khallaf *et al.*, "Investigation of aluminium and indium in situ doping of chemical bath deposited CDS thin films," *J. Phys. D, Appl. Phys.*, vol. 41, no. 18, 2008, Art. no. 185304.

[17] V. Probst *et al.*, "A new mass production technology for high-efficiency thin-film CIS-absorber formation," *IEEE J. Photovolt.*, vol. 4, no. 2, pp. 687–692, Mar. 2014.

[18] N. Naghavi *et al.*, "Buffer layers and transparent conducting oxides for chalcopyrite Cu(In,Ga)(S,Se)$_2$ based thin film photovoltaics: Present status and current developments," *Prog. Photovolt., Res. Appl.*, vol. 18, no. 6, pp. 411–433, 2010.

[19] A. O. Pudov, J. R. Sites, M. A. Contreras, T. Nakada, and H.-W. Schock, "CIGS J-V distortion in the absence of blue photons," *Thin Solid Films*, vol. 480, pp. 273–278, 2005.

[20] T. Adler *et al.*, "Valence band offsets at Cu(In,Ga)Se_2/Zn(O,S) interfaces," *Physica Status Solidi (a)*, vol. 211, no. 9, pp. 1972–1980, 2014.

Authors' photographs and biographies not available at the time of publication.